AIAA JOURNAL
Vol. 33, No. 10, October 1995

Two-Dimensional Weak Shock-Vortex Interaction in a Mixing Zone

L. Guichard,* L. Vervisch,† and P. Domingo‡
Institut National des Sciences Appliquées de Rouen, Mont-St-Aignan 76821, France

The interaction between a vortex or a pair of vortices and a shock is studied by using two-dimensional direct numerical simulation. The deformation of the shock structure is analyzed and the mechanisms leading to the formation of triple points are underscored. It is shown that they are related to the appearance of pressure gradients in the direction parallel to the shock resulting from the shock-vortex interaction. A distribution of an inert chemical species, i.e., mixture fraction, is prescribed within the vortex. From its time evolution, one analyzes the coupling between the response of the shock to the disturbance and the change in mixing rate. Modifications of the maximum of the scalar gradient are observed in the direction perpendicular to the shock and also, to a smaller extent, in the direction parallel to the shock.

Nomenclature

$A(s)$	= stretching function of the mesh
a, b, c, d	= coefficients of the PADE scheme
D	= diffusion coefficient of the inert chemical species
L	= reference length of the problem
M	= Mach number
N	= total number of grid points in streamwise direction
P	= pressure
Pr	= Prandtl number
q, q_r	= mesh stretching ratio and stretching rate
R	= radius of the vortex
Re	= acoustic Reynolds number
(r, β)	= polar coordinates
s	= position on the uniform mesh
$\boldsymbol{u}$	= velocity vector
x	= position on the nonuniform mesh
$x_{\max}$	= size of the computational domain in the streamwise direction
Y	= mass fraction of the inert chemical species (mixture fraction)
α	= coefficient of the PADE scheme
γ	= ratio of specific heats
δ_s	= shock thickness
δ_Y	= mixing layer thickness
θ	= angle characterizing the initial degree of mixing
λ	= mean free path
ρ	= density
Ψ	= stream function

Subscripts

down	= downstream from the shock wave
p	= pair of vortices
up	= upstream from the shock wave
v	= vortex
s	= singles vortex
0	= spanwise position of the mixing zone

Received Nov. 1, 1994; presented as Paper 95-0877 at the AIAA 33rd Aerospace Sciences Meeting, Reno, NV, Jan. 9–12, 1995; revision received March 15, 1995; accepted for publication March 20, 1995.

*Graduate Student, Laboratoire de Mécanique des Fluides Numérique, URA-CNRS-230-CORIA. Member AIAA.

†Associate Professor, Laboratoire de Mécanique des Fluides Numérique, URA-CNRS-230-CORIA, Place Emile blondel.

‡Research Scientist, Laboratoire de Mécanique des Fluides Numérique, URA-CNRS-230-CORIA.

Introduction

THE interaction between mixing zones and shock waves is a problem of fundamental interest. This is especially true in the case of nonpremixed supersonic combustion where the thermodiffusive balance, which controls the inner structure of the flame, may be strongly modified by pressure discontinuities.[1] Within supersonic reactive mixing layers, coherent structures, which play a crucial role in mixing, can be convected through shock waves. Therefore, quantifying the impact of a pressure discontinuity on the properties of the structure itself and on the degree of mixing is of importance in characterizing supersonic combustion systems.

In this spirit, we have carried out two-dimensional numerical simulations to investigate the interaction between a vortex or a pair of vortices and a weak shock wave. The effect of the shock on mixing is addressed by prescribing within the vortex a distribution of a nonreactive species Y which will be convected through the shock interface; here, Y characterizes the mixing and corresponds to the mixture fraction widely used in the description of nonpremixed turbulent flames.[1] The time evolution of the mixture fraction gradients in both the parallel and perpendicular directions to the shock are indicators of the modification of mixing which could be induced by the presence of pressure discontinuities.

We have essentially restricted the study to weak shocks because this allows us to solve the inner structure of the shock without adding any artificial numerical treatment. Consequently, it enables the examination in great detail of the local deformation of the shock, along with the corresponding effect on the vortices when they travel from supersonic zones to subsonic zones. Moreover, weak shocks are known to be an effective concept when one wishes to investigate thoroughly the behavior of pressure jumps in flows.[2]

The tone in the following is mostly descriptive; the results are issued from observation of the numerical results. The properties of the shock wave and of the structure of the vortices during their interaction are described in detail, and it is found that the shock interface is first locally stretched by the vorticity and then secondary pressure discontinuities appear. They result from the deformation of the shock, which yields to a nonzero value of the component of the pressure gradient in the direction parallel to the shock. These waves are induced by the circulation of the vortex, and they are attached to the shock. By increasing the vorticity magnitude, it is observed that these secondary pressure jumps can become shock waves before the shock relaxes to its initial steady condition. With regard to mixing rate modification, it is observed that the component of the mixture fraction gradient in the direction normal to the shock is increased by compression, whereas the local deformation of the shock plus the rotation of the vortex, which convects the increase in the normal direction, are responsible for the enhancement of the parallel component of this gradient.

Finally, in the case of a pair of vortices, a simple analysis emerges from the observed features of the acoustic field. It is based on the extrapolation of the phenomena observed in the single vortex situation.

Methodology

The fully compressible Navier–Stokes equations are solved, the Schmidt number and the Prandtl number are constant and the dynamic viscosity is a function of the temperature. Figure 1 is a sketch of the simulation, at the supersonic entrance, where constant values for the mass flow rate, density and total energy are prescribed, whereas nonreflecting boundary conditions[3] are used at the subsonic outlet and at the spanwise boundaries of the computational domain.

A sixth-order accurate PADE spatial discretization[4] is jointly used with a third-order accurate Runge–Kutta method for time stepping,[5] and the present simulations are two dimensional. This numerical approach has been shown to be an effective tool for studying shock-turbulence interaction.[6] The first derivative of a quantity f, evaluated on a mesh constituted of N grid nodes equally separated by a distance Δs, is for the finite difference Lele's quasispectral scheme[4]:

$$f'_i + \alpha(f'_{i+1} + f'_{i-1}) = \frac{a}{2\Delta s}(f_{i+1} - f_{i-1}) + \frac{b}{4\Delta s}(f_{i+2} - f_{i-2})$$

When introducing Taylor series expansion this becomes

$$f'_i = \sum_{n=0}^{\infty} f_i^{2n+1} \Delta s^{2n} \left(\frac{a + 2^{2n} b}{(2n+1)!} - \frac{2}{(2n)!}\alpha \right)$$

From the preceding expression one deduces[4] the values of the coefficients α, a, and b which provide an approximation for the point $3 < i < N - 2$ that is sixth-order accurate

$$\alpha = \tfrac{1}{3}, \qquad a = \tfrac{1}{3}(4 - 2\alpha), \qquad b = \tfrac{1}{3}(4\alpha - 1)$$

At the boundaries ($i = 1, i = N$) the accuracy is reduced to third order, although a fourth-order scheme that ensures conservative properties is chosen for the points $i = 2$ and $i = N - 1$.

The same procedure is applied to get a finite difference approximation of the second-order derivative

$$f''_i + \alpha(f''_{i+1} + f''_{i-1}) = \frac{1}{\Delta s^2}\left[a(f_{i+1} - 2f_i + f_{i-1}) + \frac{b}{4}(f_{i+2} - 2f_i + f_{i-2}) \right]$$

leading to

$$f''_i = \sum_{n=1}^{\infty} f_i^{2n} \Delta s^{2n-2} \frac{2}{(2n)!}\left[a + 2^{2n-2} b - \frac{(2n)!}{(2n-2)!}\alpha \right]$$

and sixth-order accuracy is obtained for

$$\alpha = 11, \qquad a = 13, \qquad b = -27, \qquad c = 15, \qquad d = -1$$

Derivatives are evaluated by projection of the nonuniform mesh ($0 < x < x_{\max}$) on to a regular mesh ($0 < s < 1$), which step is Δs. The nonuniform mesh is generated by imposing a stretching position x_0, a stretching ratio q, and a stretching rate q_r. The link between the s and x coordinates is given by

$$x = [x_{\max}/A(1)]A(s)$$

where

$$A(s) = s - \frac{\sqrt{\pi}}{2}\frac{q}{q_r}\{\operatorname{erf}[q_r(s - s_0)] - \operatorname{erf}(-q_r s_0)\}$$

and the s_0 parameter is obtained from the solution of

$$s_0 = \frac{x_0}{x_{\max}} A(1) - \frac{\sqrt{\pi}}{2}\frac{q}{q_r}\operatorname{erf}(-q_r s_0)$$

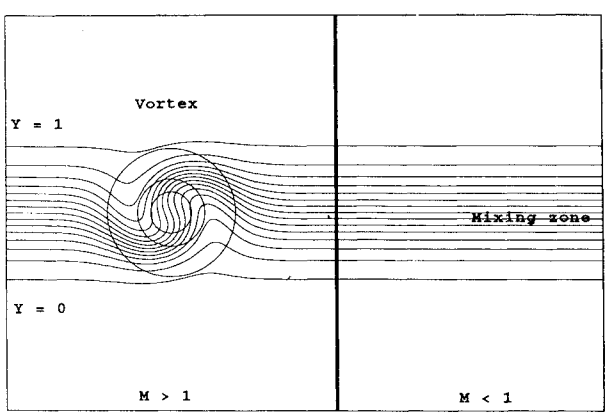

Fig. 1 Sketch of the simulation.

First a one-dimensional shock configuration is computed to estimate the numerical accuracy and to initialize the two-dimensional simulations. This preliminary simulation is initiated by using the Rankine–Hugoniot relations and the prescribed distributions for pressure and density inside the shock. A first guess of the shock's thickness is given by using the relations of Shapiro[8]

$$\delta_s \simeq \frac{4}{\gamma + 1}\left(\frac{4}{3} + \frac{\gamma - 1}{Pr}\right)\frac{1}{Re(M^* - 1)}$$

where

$$M^{*2} = \frac{[(\gamma + 1)/2]M_{\text{up}}^2}{1 + [(\gamma - 1)/2]M_{\text{up}}^2}$$

where M_{up} is the inlet Mach number. This is found to provide the thickness of the shock within a 7% accuracy compared to the converged one-dimensional solution. The weak shock resulting from the one-dimensional solution displays stable profiles in time and is used to initialize the problems.

A vortex characterized by the stream function Ψ and the pressure distribution $P(r)$ (Ref. 9) is added to the supersonic side:

$$\Psi = u^v R \exp\left(\frac{1}{2} - \frac{r^2}{2R^2}\right), \qquad P(r) = P_\infty - \frac{\rho}{2R^2}\Psi^2$$

where R is the radius of the vortex and u^v the maximum value of its tangential velocity.

The conservation equation subject to the concentration level $Y(\underline{x}, t)$ of the mixture fraction may be written

$$\frac{\partial Y}{\partial t} = -\boldsymbol{u} \cdot \nabla Y + \frac{1}{\rho}[\nabla(\rho D \nabla Y)]$$

As an initial condition, a hyperbolic tangent distribution with a gradient parallel to the shock is chosen for Y

$$Y(x, y) = \frac{1}{2}\left\{1 - th\left[\frac{2(y^v - y_0)}{\delta_Y}\right]\right\}$$

where y_0 is the spanwise position of the mixing zone, δ_Y its thickness, and y^v the distribution within the vortex, which is organized such that

$$y^v = y_0^v + r \sin\left[\beta - \theta \exp\left(\frac{1}{2}\frac{1 - r}{R^2}\right)\right]$$

where the polar coordinates (r, β) are defined relative to the position of the core of the vortex (x_0^u, y_0^v). The θ angle controls the initial degree of mixing. This distribution provides gradients of the mixture fraction field in all of the spatial directions and will be convected by the flowfield toward the shock wave. Various values for the magnitude of the gradient along the isolines of the mixture fraction field associated with a distribution of strain rate will then interact with the pressure discontinuity.

The Navier–Stokes equations are solved in nondimensional form. To characterize the considered problem, it is possible to relate the acoustic Reynolds number Re, based on the speed of sound, and a

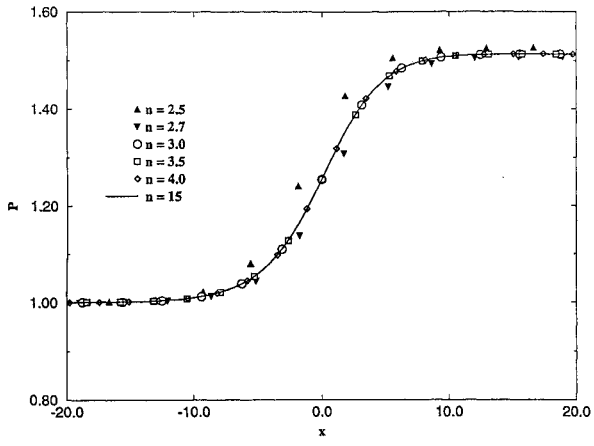

Fig. 2 One-dimensional weak shock computations for various grid refinements, $n = N\delta_s/x_{max}$.

characteristic length of the study (L) to the mean free path λ. By using the relationship between the dynamic viscosity and the mean free path[10] one may write $Re/2 \sim L/\lambda$. The thickness of the weak shock is on the order of 10 mean free paths, whereas the diameter of the vortex is equivalent to 250λ (the computational domain contains 2000λ). The inlet Mach number M_{up} is set to 1.2, whereas the value of the pressure and density are those of the standard conditions. Results are made nondimensional by the inlet Mach number and by the thickness of the shock evaluated as

$$\delta_s = \left[(P_{down} - P_{up}) / \max\left(\frac{\partial P(x)}{\partial x} \right) \right]$$

where P_{up} and P_{down} are the upstream and downstream value of the pressure. In this nondimensional shock unit system, the length of the computational domain is $x_{max} = 2000$, and the mesh is refined at the shock location with the parameters $q = 23$ and $q_r = 77$. The mesh is also refined in the transverse direction (direction of the mean mixture fraction gradient) at the position y_0 ($q = 21$ and $q_r = 38$). The simulations are realized with a 256×192 mesh. (Each of the presented simulations represents a CPU time of about 4 h on a SGI Challenge L.) To determine this optimal set of parameters tests have been performed with various grid refinements. Figure 2 displays pressure profiles in the case of one-dimensional shock computations corresponding to different numbers of grid points within the shock interface, oscillations have been observed for coarse grids, i.e., $n = N\delta_s/x_{max} < 3$. Hence, the stretching parameters for the two-dimensional computations have been chosen in order to always ensure $n > 3$ in the zones where pressure discontinuities need to be captured.

The vortices are characterized by the maximum velocity u^v they induce and by a length l^v estimated, in the case of a single vortex, like the diameter of the vortex, or, in the case of a pair of vortices, like the sum of the diameter and the distance between the core of the vortices. The single vortex is characterized in shock units by a length $l_s^v = 25$ and a velocity $u_s^v = 0.33$, whereas the pair of vortices corresponds to $l_p^v = 50$ and $u_p^v = 0.33$. The mixing layer's thickness is equal to $\delta_Y = 40$ in shock units.

Shock-Single Vortex Interaction

When the vortex interacts with the shock, the velocity field of the vortex is added to the jump in velocity imposed by the shock interface, and the discontinuity is convected toward the subsonic zone by the higher streamwise velocity $U_{up} + u^v$ induced by the vortex and toward the supersonic zone by the lower streamwise velocity $U_{up} - u^v$ (Fig. 3a). Thus, the pressure discontinuity interacting with the vortex is symmetrically stretched at first (Fig. 4). The additional velocity ($+u^v$) is responsible for the creation of a stronger shock zone with an increase in pressure of $(1/2)\rho u^{v2}$. Similarly, a weaker shock is formed by the decrease in velocity $-u^v$. Because of the different values of the pressure jump along the shock in the spanwise direction, the vortex is distorted (Fig. 4). This goes along with a nonsymmetric deformation of the shock featuring a more

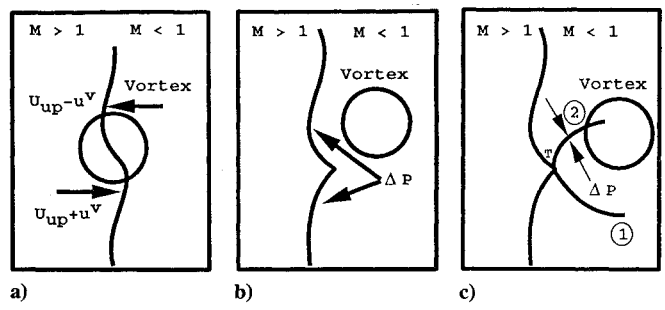

Fig. 3 Sketch of the shock-single vortex interaction.

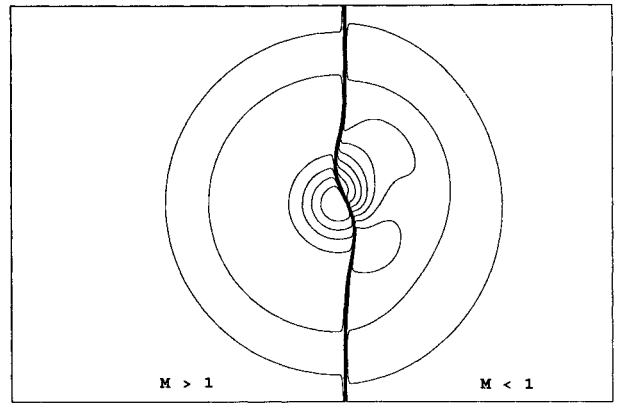

Fig. 4 Pressure field: vortex crossing the shock.

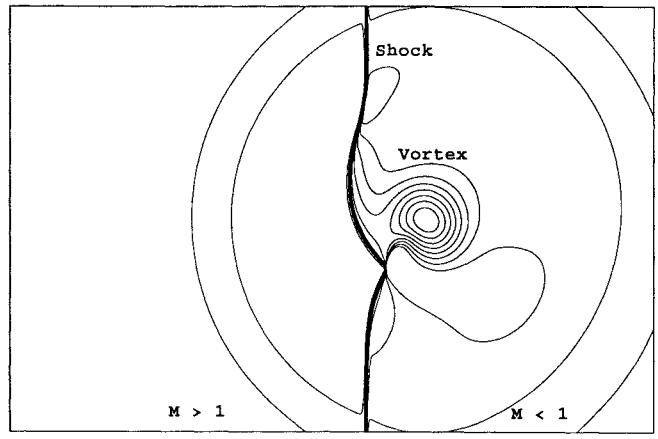

Fig. 5 Pressure field: vortex in subsonic zone.

pronounced curvature in the subsonic side (Fig. 5) that evolves into a cusp. During this deformation, pressure gradients appear in the transverse direction (Figs. 6 and 3b). These additional transverse components to the pressure jump locally generate secondary pressure discontinuities visible in Fig. 6 and noted 1 and 2 in Fig. 3c. They are both attached to the shock. The secondary discontinuity 1 follows the circulation of the vortex and decays as the structure moves away from the shock. The upper branch 2 touches the vortex and is sustained by its rotation (Fig. 3c). It is observed that for small values of the vorticity the shock relaxes to its initial position before the convected compression zone 2 can become an entropy jump; in the case of a stronger vortex this wave may behave like a secondary shock leading to a triple point, noted T in Fig. 3. For successive times, Fig. 7 presents longitudinal pressure profiles in the shock zone at a spanwise location corresponding to the position of the cusp where a triple point may be found. One may observe the initial condition (t_0), the displacement of the shock along with the local compression (t_1) and the relaxation of the shock interface toward its initial position (t_2 and t_3).

In all of the figures presenting the pressure field, circular pressure waves generated by the relaxation of the incompressible initial

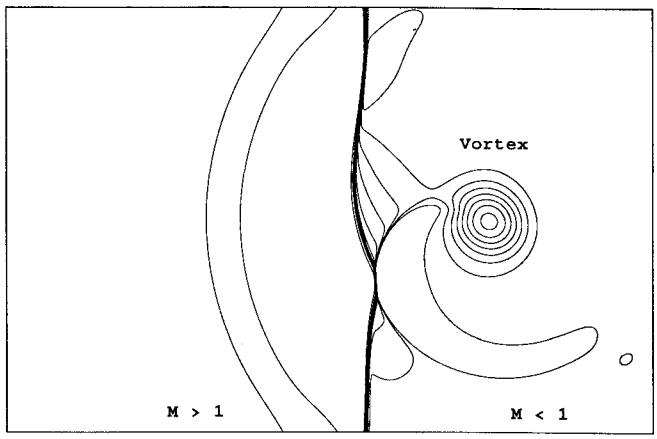

Fig. 6 Pressure field: vortex in subsonic zone.

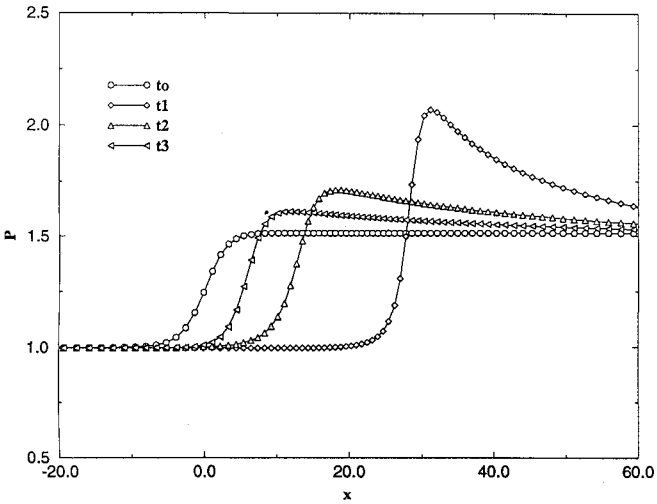

Fig. 7 Time evolution of the longitudinal pressure profiles at location T; see Fig. 3.

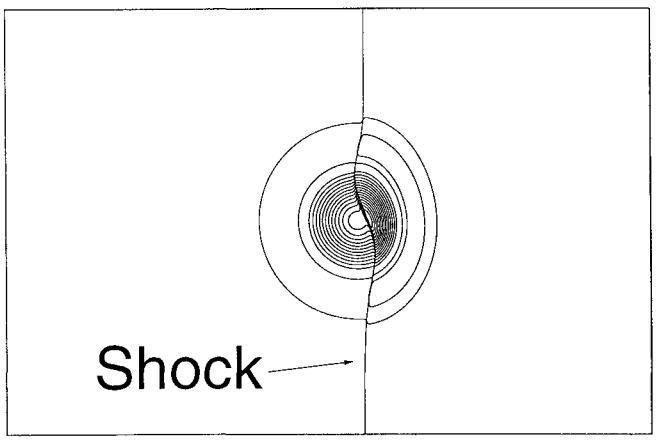

Fig. 8 Vorticity field: vortex crossing the shock.

vortex condition are visible, and within the core of the vortex, the pressure distribution due to the vortex motion is also observed. Because of the compressibility effects, the vorticity magnitude is increased and the structure is compressed in the direction normal to the shock (Fig. 8), and it is bent according to the curvature of the shock (Fig. 9).

We now wish to focus on the impact of the shock on the structure of the mixing zone. The gradient of the mixture fraction is modified by compression; maximum values of its components in both directions normal (x) and parallel to the shock (y) are plotted vs time in Fig. 9. First, it is important to note that the mean slopes of the curves $\max[\nabla_x Y(t)]$ and $\max[\nabla_y Y(t)]$ (Fig. 10) are controlled by the relative effects of diffusion and convection, therefore, only

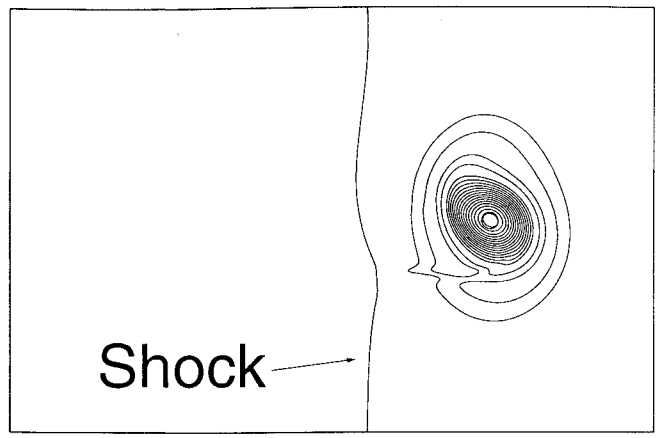

Fig. 9 Vorticity field: vortex in subsonic zone.

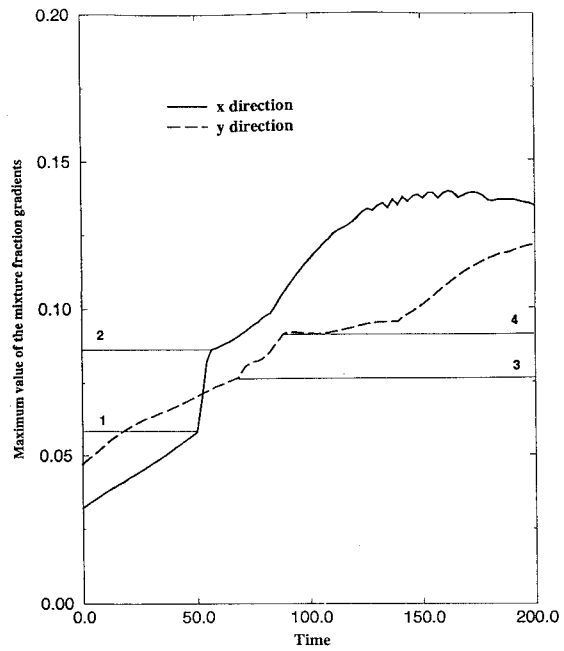

Fig. 10 Time evolution of the maximum value of the components of the mixture fraction gradients, x direction normal to the shock, and y direction parallel to the shock.

sudden evolutions are relevant to quantify mixing rate modifications that are directly linked to the presence of the shock.

A jump is observed for $\max[\nabla_x Y(t)]$ when the vortex interacts with the pressure discontinuity (from 1 to 2 in Fig. 10). Because of the movement induced by the vortex, the value of this jump is found to be larger ($\sim$10%) than the order of magnitude evaluated in a one-dimensional compression of the nonreactive mixture fraction field. This modification of the gradient is convected by the circulation of the vortex and yields to an increase in the direction parallel to the shock. Moreover, the nonsymmetric deformation of the shock interface already mentioned brings for the mixture fraction a convective lag between the stronger and the weaker shock zones [Figs. 3a and 3b]. This phenomenon, in conjunction with the appearance of a pressure gradient in the y direction, explains the increase of $\max[\nabla_y Y(t)]$ observed in Fig. 10 (from 3 to 4).

Therefore, the gradients of the scalar field both in directions parallel and perpendicular to the shock are increased during the shock-structure interaction and so is diffusion at the scale of the vortex.

Shock-Pair of Vortices Interaction

In supersonic flows involving complex geometries, when vortical structures and shock waves are simultaneously present, it is likely that mixing zones feature multiple shock-vortices interactions. In this section we describe the interaction between a weak shock and

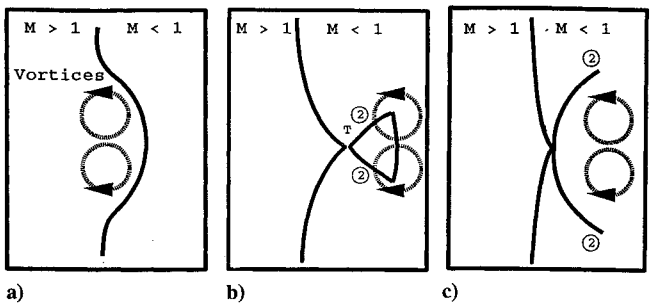

Fig. 11 Sketch of the shock-pair of vortices A interaction.

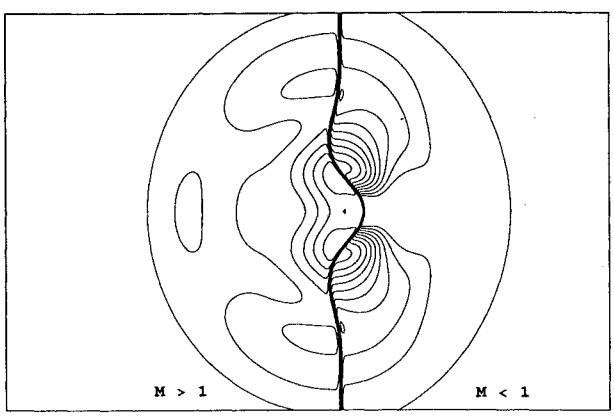

Fig. 12 Pressure field: vortices A crossing the shock.

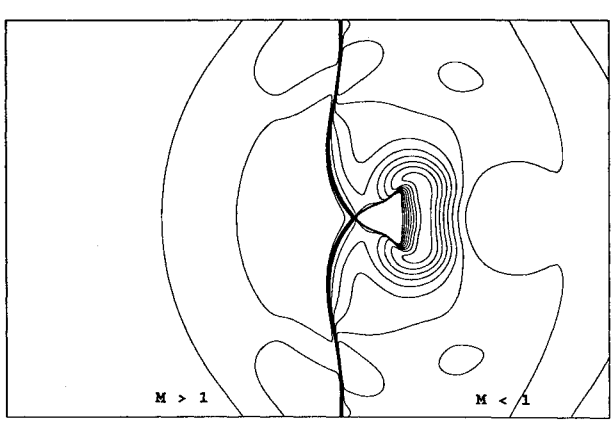

Fig. 13 Pressure field: pair of vortices A in subsonic zone.

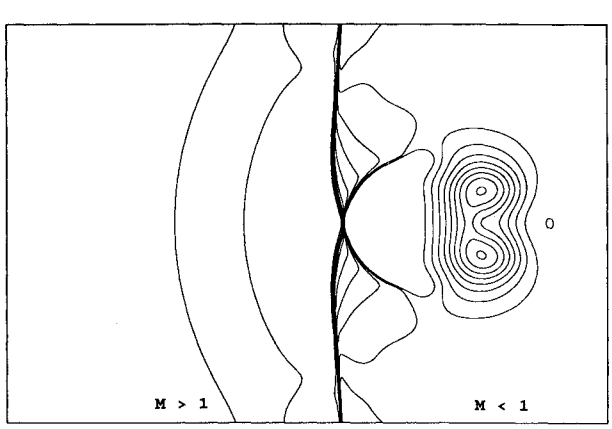

Fig. 14 Pressure field: pair of vortices A in subsonic zone, relaxation of the shock.

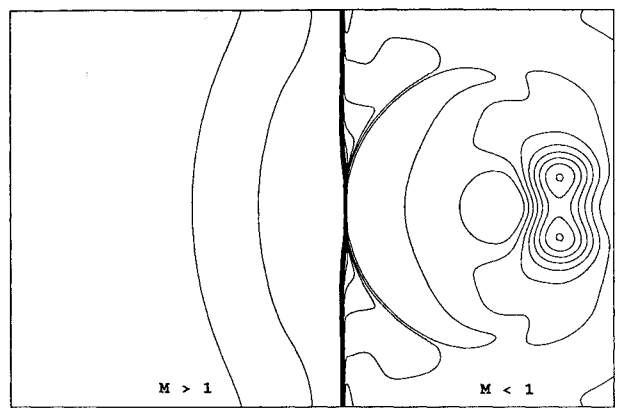

Fig. 15 Pressure field: pair of vortices A in subsonic zone, exiting the computational domain.

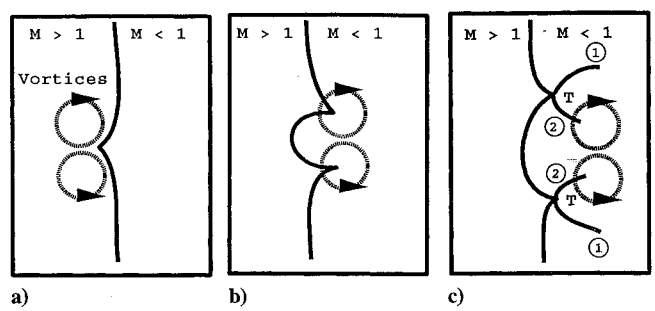

Fig. 16 Sketch of the shock-pair of vortices B interaction.

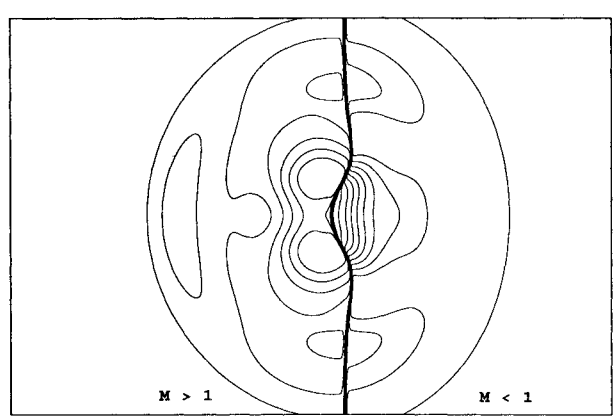

Fig. 17 Pressure field: pair of vortices B crossing the shock.

a pair of vortical structures. Two vortices are convected toward the shock and, depending on the relative orientation of their vorticity vectors, the possibilities of generating one or two triple points emerge.

Figure 11 is a sketch of the pair of vortices-shock interaction corresponding to the case of two vortices rotating so that the velocities they induced are added to push the shock interface toward subsonic zone (case A). Figure 12 shows the deformation of the shock toward the subsonic zone; then a cusp is formed (Figs. 11b and 13) and two secondary pressure discontinuities appear. These waves are equivalent to the upper pressure jump observed in the single vortex interaction (Fig. 3c). As observed in Fig. 13, the secondary pressure jumps 2 following local depressions are sustained by the rotation of the vortices and lead, when they merge, to the possibility of a single triple point (denoted T in Fig. 11b). The compression, i.e., creation of a stronger shock, is simply convected by the pair of vortices; therefore, waves equivalent to 1 of Fig. 3c cannot exist. Then the system relaxes (Figs. 14 and 15).

Figure 16 is a sketch of the pair of vortices-shock interaction corresponding to the case of two vortices rotating so that the velocities

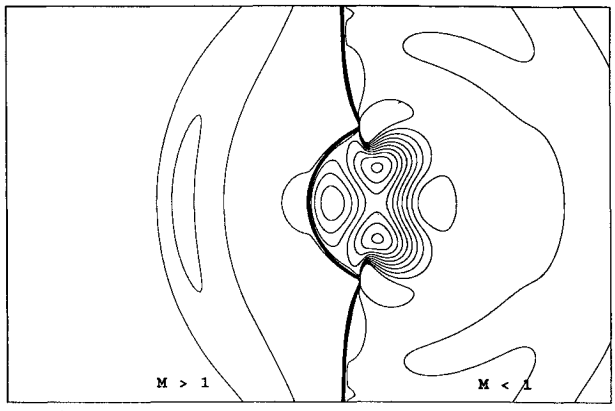

Fig. 18 Pressure field: pair of vortices B in subsonic zone.

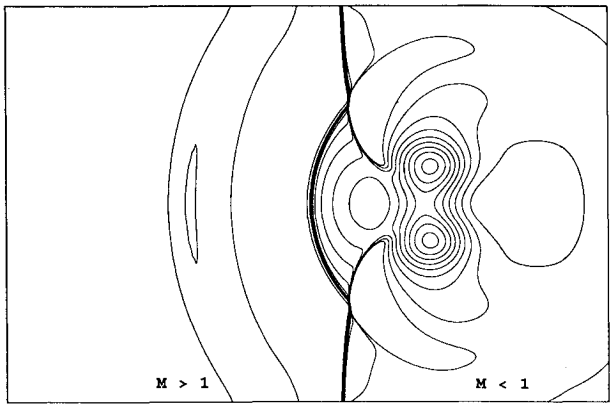

Fig. 19 Pressure field: pair of vortices B in subsonic zone, relaxation of the shock.

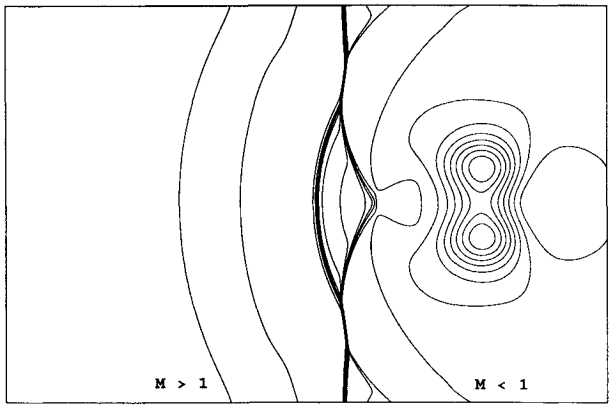

Fig. 20 Pressure field: pair of vortices B in subsonic zone, exiting the computational domain.

they induced are subtracted to the upstream velocity to attract the shock interface to the supersonic zone (case B). At a first stage, the shock is convected upstream by the vortices (Figs. 16a and 17). Then, each vortex induces a cusp (Figs. 16b and 18). From each cusp, two secondary pressure discontinuities develop (Figs. 16c and 19) two triple points are formed. Figure 20 shows the relaxation of the shock with the two secondary shocks 2 merging. In this case (Figs. 16–20) the interaction behaves like a double single vortex-shock interaction.

Conclusion

Within supersonic combustion devices, mixing zones involving large-scale structures and shock waves interact. We have thoroughly investigated the interaction between a weak shock wave and a vortex and/or a pair of vortices convecting an inert mixing zone. Direct numerical simulations including viscous effects have been performed, and various physical phenomena linked to the modification of the shock and to the mixing zone are observed.

The generation of acoustic waves is found and is associated with a nonsymmetric deformation of the shock structure. During the interaction, pressure gradients in the direction parallel to the shock are created. They promote the generation of two secondary pressure discontinuities attached to the shock, and one of them may lead to the existence of a triple point.

An increase in the maximum value of the scalar gradient induced by the crossing of the pressure discontinuity is shown to be present in both components of the gradient, parallel and perpendicular to the shock.

The possible formation of triple points, which is a very important feature of supersonic-subsonic transition, has been observed in all of the studied interactions.

References

[1]Marble, F. E., Hendricks, G. J., and Zukoski, E. E., "Progress Toward Shock Enhancement of Supersonic Combustion Processes," AIAA Paper 87-1880, July 1987.

[2]Tabak, E. G., and Rosales, R. R., "Focusing of Weak Shock Waves and the von Neumann Paradox of Oblique Shock Reflection," *Physics of Fluids*, Vol. 6, No. 5, 1994, pp. 1874–1892.

[3]Poinsot, T., and Lele, S. K., "Boundary Conditions for Direct Simulations of Compressible Viscous Flows," *Journal of Computational Physics*, Vol. 101, No. 1, 1992, pp. 104–129.

[4]Lele, S. K., "Compact Finite Difference Schemes with Spectral Like Resolution," Center for Turbulence Research Rept., Stanford Univ., Stanford, CA, 1990.

[5]Wray, A. A., "Minimal Storage Time-Advancement Schemes for Spectral Methods," Center for Turbulence Research Rept., Stanford Univ., Stanford, CA, 1990.

[6]Lee, S., Lele, S. K., and Moin, P., "Direct Numerical Simulation of Isotropic Turbulence Interacting with a Weak Shock Wave," *Journal of Fluid Mechanics*, Vol. 251, June 1993, pp. 533–562.

[7]Struminskii, V. V., and Velikodnyi, V. Y., "Structure of Shock Waves," *Soviet Physics—Doklady*, Vol. 27, No. 9, 1982, pp. 659–661.

[8]Shapiro, A. H., "The Dynamics and Thermodynamics of Compressible Fluid Flow," Ronald, New York, 1953.

[9]De Neufville, A., "The Dying Vortex," *Proceedings of the Fifth Midwestern Conference on Fluid Mechanics*, University of Michigan, 1957, p. 365.

[10]Thompson, P. A., *Compressible-Fluid Dynamics*, Advanced Engineering Series, edited by I. H. Shames, 1988, Chap. 2.